Development of a global non-hydrostatic simulation code using Yin-Yang grid system

*Kenji Komine, Keiko Takahashi, Kunihiko Watanabe (Earth Simulator Center, Japan Agency for Marine-Earth Science and Technology.)
E-Mail: komine@jamstec.go.jp

Introduction

For the purpose of high-resolution atmospheric simulations, we have been developing new global non-hydro -static atmospheric simulation code using a kind of overset grid, named Yin-Yang grid system (1) on the sphere (Fig. 1). Yin-Yang grid system was developed in Solid Earth Simulation Group of the Earth Simulator Center. By having this new grid system, we could avoid a problem of how to cover the South Pole and North Pole, and enlarge the time step of simulation compared to the commonly utilized latitude/longitude grid system. Each system of component grid covers a lower latitude part of the latitude-longitude grid. In this presentation, we indicate numerical implementations and show the results of fundamental mountain wave propagation experiments (2) (3) for the validation of effects of metric terms and of benchmark tests with Held and Suarez forcing (1994) (4) for the validation of long-term integration.

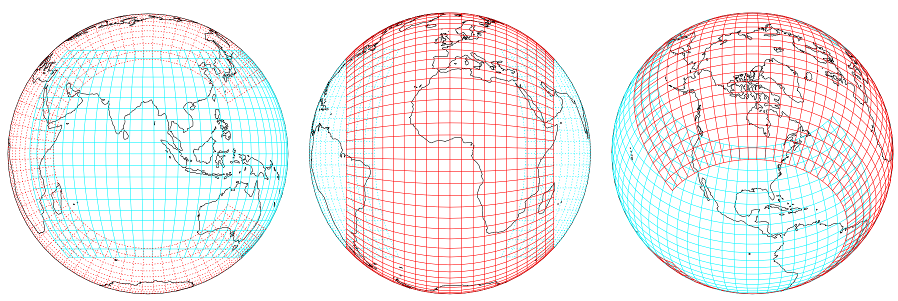

(a) N-System (blue) (b) E-System (red) (c) Yin-Yang grid (N-System + E-System)

Fig.1. Yin-Yang grid system

Governing equations and Numerical method

We solve fully compressive three-dimensional Naiver-Stokes equations with rotational effects, continuity equation, pressure equation and the equation of the state. Numerical schemes of this simulation code are shown in Table 1.

$$\frac{\partial \rho'}{\partial t} + \nabla \bullet (\rho \mathbf{v}) = 0 \qquad \rho' = \rho - \overline{\rho} \ \text{: perturbation density}$$

$$\frac{\partial \rho \mathbf{v}}{\partial t} + \nabla p' + \rho' \mathbf{g} = -\nabla \bullet (\rho \mathbf{v}\mathbf{v}) + 2\rho \mathbf{v} \times \mathbf{f} + \mathbf{F} \qquad \rho\mathbf{v} \ \text{: momentum,} \ \mathbf{v} = (u, v, w) \ \text{: velocity}$$

$$\frac{\partial P'}{\partial t} - \overline{\rho}\mathbf{g}w + \mathbf{v}\nabla P' + \gamma P \nabla \mathbf{v} = (\gamma - 1)\kappa \nabla^2 T + (\gamma - 1)\Phi \qquad P' = P - \overline{P} \ \text{: perturbation pressure}$$

$$P = \rho R T$$

$\mathbf{f}, \mu, \kappa, \gamma, \Phi, \mathbf{F}$: Coriolis parameter, viscosity coefficient, diffusion coefficient, ratio of heat capacities, heating term, viscous term

Table1. Numerical methods in the simulation code.

Item		Contents
The equation system		Fully compressible Navier-Stokes equations
Grid system	Horizontal	Yin-Yang grid, spherical coordinate system(1)
	Vertical	Z^* coordinate system
Discretization	Horizontal	Arakawa-C grid, 2nd order FDM and 5th order FDM(5)
	Vertical	Lorenz grid, 2nd order FDM and 5th order FDM(5)
Time integration		HE-VI (Horizontally Explicit- Vertically Implicit) 3rd order RungeKutta (large time step) (5) Forward-Backward (small time step)
Boundary condition	Upper & Lower	$w^*=0$, free slip for u and v.
	Lateral (for Yin-Yang grid).	3rd order Lagrange interpolation Global mass conservative interpolation scheme (6) $\int_{\Gamma_{EN}} f_E d\Gamma = \int_{\Gamma_{NE}} f_N d\Gamma$: the conservation condition Γ_{NE}, Γ_{EN} : Boundary of N or E system, f_N, f_E : mass flux on the lateral boundary
Numerical stabilization		Divergence damping, 2nd order numerical viscosity, Rayleigh damping for momentum
Parallelization		2-D decomposition with MPI and Mircotask.

Computational performance

The simulation code has attained about 60 percent of theoretical peak performance of the Earth Simulator with 512 nodes (Table 2). Fig.2 shows performance statistics of our code with different horizontal resolution on the Earth Simulator. Those results confirm high computational performance and high parallelization ratio of this code.

Table 2. Computational performance of the simulation code on the Earth Simulator.

Resolution [km]	grid points	# of nodes	Peak perf. ratio [%]	Vec. op. ratio [%]	Vec. length
20.9	1440x480x96x2	6	58.1	99.53	236.8
10.4	2880x960x96x2	24	56.7	99.52	237.4
5.2	5760x1920x96x2	96	59.9	99.54	239.2
3.5	8640x2880x96x2	216	60.0	99.54	238.9
2.6	11520x3840x96x2	512	59.9	99.60	239.7

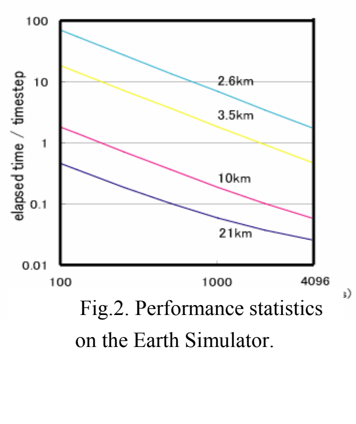

Fig.2. Performance statistics on the Earth Simulator.

Mountain waves experiments

The purpose of this test is to verify the accuracy of the metric term resulting from the non-orthogonality of the vertical grid and the interpolation effect of the Yin-Yang grid. Following Qian et al. (1998) and Tomita and Sato (2004) (2) (3), we examine the characteristics of the numerical solutions associated with a simple isolated mountain.

・The height of the top of the code is 40 km and uses 24 vertical layers equally spaced in z^*.

・We set the mountain height h =1000m and the half-width d =1250km .

・The Brunt-Vaisala frequency is N=0.0187 s^{-1} .

・Set uniform zonal mean easterly flow of u = -40cosϕ m s^{-1}.

・Rayleigh damping layer are set from top to 2/3 height for $\rho u, \rho v, \rho w$.

In order to consider the influence of the boundary interpolation between the component grid, we performed two experiment using the same setup without the mountain location as (0N, 180E) or (0N, 45W).

Geographical feature has arranged the bell type mountain consisting mainly of (0N, 180E).

The location (0N, 45E) is correspond to the boundary of the Yin-Yang grid. An isolated bell-shaped mountain with different locations is employed.

Fig. 2 (a) shows vertical cross section of vertical speed w. The mountain waves spread toward the upper layer. (b) also shows the divergence at 10km height. Fig. 3 shows the results with the mountain location as (0N, 45W). From these results, we verified that integral was possible without influence of the overlap portion of the Yin-Yang grid, although the center of mountain sets the boundary of each component grid.

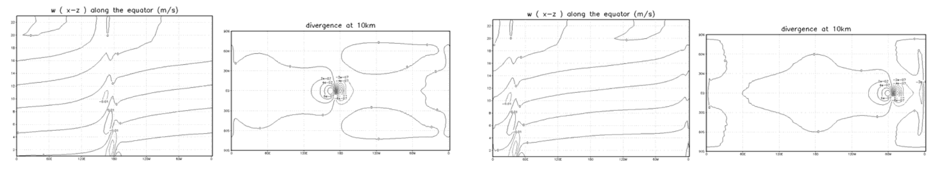

(a) (b) (a) (b)

Fig.3. (a) The snapshot of λ-z cross section of vertical wind speed w (m s^{-1}) along the equator at day 30. (b) The snapshot of horizontal divergence at 10km at day 30. The mountain location is (0N, 180E).

Fig.4. As in Fig 2 except the mountain location as (0N, 45W).

Held and Suarez experiment

In order to verify long-term statistical properties of a fully developed general circulation, a benchmark calculation proposed by Held and Suarez(1994) were performed. Held and Suarez (1994) gave easy external force for conducted dynamic equation and pressure equation. Fig. 5 shows distribution of zonal mean temperature. Fig. 6 presents average for 1000 days of the zonal mean zonal wind produced by our simulation code Single jet near 45N and lower layer wind velocity profile was comparable with previous results. It is also shown that systematic noise is not seen on 45N, near boundary of overset grid. Because numerical stabilization schemes are not equal to original paper, we shall tune coefficients of viscosity and diffusion in order to improve the results. These results show that this simulation code can perform without influence of interpolation on the boundary for long-term integration. Total mass may conserve $O(10^{-13})$ in this simulation.

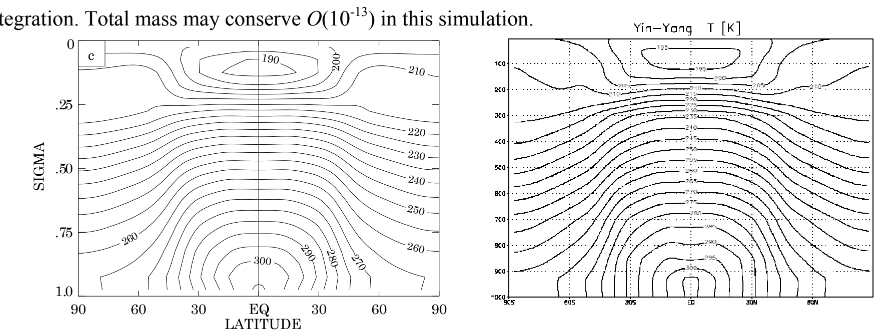

(a) (b)

Fig.5 The zonal mean temperature T [K] (a) Held and Suarez, (b) produced by the code using Yin-Yang grid.

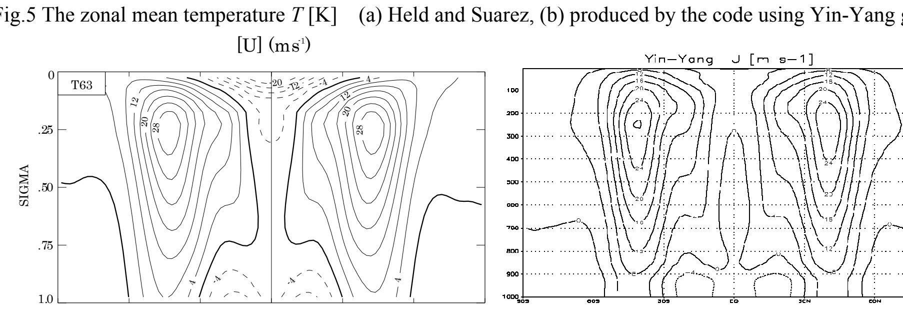

(a) (b)

Fig.6 The zonal mean zonal wind U [m sec-1] (a) Held and Suarez, (b) produced by the code using Yin-Yang grid.

Future works

In order to progress this simulation code, we will apply higher order advection scheme and an interpolation scheme as in Peng et al. (2004)(7) . Smagorinsky first-order turbulence closure scheme and surface flux scheme will be implement. We will perform simulations with high resolution (up to 2.6km) to reproduce wind fields with the realistic geometry.

References

(1) Kageyama, A., Sato, T., 2003: The "Yin-Yang Grid": An Overset Grid in Spherical Geometry, to be published *Geochem. Geophys. Geosyst.*, E-print: physics/0403123.

(2) Qian, J. H., Semmazzi, F. H. M., Scroggs, J.S., 1998: A globl nonhydrostatic semi-lagrangian atmospheric model with orography. *Mon. Wea. Rev.* 126, 747-771.

(3) Tomita and Satoh, 2004: A new dynamical framework of nonhydrostatic global model using the icosahedral grid, *Fluid Dynamics Research*, 34, 357-400pp.

(4) Held, I. M., Suarez, M. J., 1994: A proposal for the intercomparison of the dynamical cores of atmospheric general circulation models. *Bull. Am. Meteorol. Soc.* 75, 1825-1830.

(5) Wicker, L. J., Skamarock, W.C., 2002: Time-splitting methods for elastic models using forward time schemes. *Mon. Wea. Rev.* 130, 2088-2097. (5) Berger, M. J., 1987: On Conservation At Grid Interfaces, *SIAM J. NUMER. ANAL.* 24, 967-984.

(6) Berger, 1987: On Conservation At Grid Interfaces, *SIAM J. NUMER. ANAL.*, 24, 967-984.

(7) Peng, X., Xiao, F., Takahashi, K.: Application of the CIP-CSLR on the ``Yin-Yang Grid'' in spherical geometry. The 2004 Workshop on the Solution of Partial Differential Equations on the Sphere, pp21.